

Novel Therapeutic Agents for Bone Resorption. Part 1. Synthesis and Protonation Thermodynamics of Poly(amido-amine)s Containing Bis-phosphonate Residues

Mario Casolaro* and Ilaria Casolaro†

Dipartimento di Scienze e Tecnologie Chimiche e dei Biosistemi, Università di Siena, Via Aldo Moro 2, I-53100 Siena, Italy

Adriano Spreafico, Caterina Capperucci, Bruno Frediani, and Roberto Marcolongo
Sezione di Reumatologia, Dipartimento di Medicina Clinica e Scienze Immunologiche, Università di Siena, Policlinico "Le Scotte", I-53100 Siena, Italy

Nicola Margiotta and Rosa Ostuni

Dipartimento Farmaco-Chimico, Università di Bari, Via Orabona 4, I-70125 Bari, Italy

Raniero Mendichi

Istituto per lo Studio delle Macromolecole (CNR), Via E. Bassini 15, I-20133 Milano, Italy

Filippo Samperi

Istituto di Chimica e Tecnologia dei Polimeri, Sez. Catania (CNR), Dipartimento di Chimica, Università di Catania, Viale A. Doria 6, I-95125 Catania, Italy

Takehiko Ishii

RIKEN (The Institute of Physical and Chemical Research), Hirosawa 2-1, Wako, Saitama, 351-0198, Japan

Yoshihiro Ito

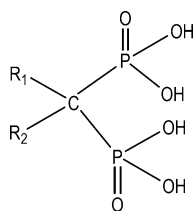
Kanagawa Academy of Science and Technology, KSP East 309, Sakado 3-2-1, Takatsu-ku, Kawasaki, Kanagawa 213-0012, Japan, and RIKEN (The Institute of Physical and Chemical, Research), Hirosawa 2-1, Wako, Saitama 351-0198, Japan

Received August 4, 2006; Revised Manuscript Received September 12, 2006

Two poly(amido-amine)s (oligoPAM and oligoNER) containing bis-phosphonate residues were obtained by a Michael-type polyaddition of pamidronate and neridronate to 1,4-bis(acryloyl)piperazine. The SEC (size-exclusion chromatography) and the MALDI-TOF (matrix assisted laser desorption ionization) analyses were consistent with the presence of oligomeric species (2–3 kDa) and with a narrow polydispersity index. The thermodynamic results ($\log K_s$, $-\Delta H^\circ$, and ΔS° obtained at 25 °C in 0.15 M NaCl) of both the oligomers and the corresponding low molecular weight precursors were in line with a cluster structure formed during the protonation of the basic nitrogen in the pamidronate. The solubility of the oligoNER with a longer aliphatic chain was improved at high pHs, allowing the evaluation of their solution properties. Preliminary biological results show that both the oligomers do not negatively affect the in vitro viability, proliferation, and cellular activity of either normal animal or human osteoblasts.

Introduction

Bis-phosphonates (BPs) are synthetic drugs based on a phosphorus–carbon–phosphorus template, structurally related to endogenous pyrophosphates. Besides the resistance to enzymatic and chemical hydrolysis, the P–C–P carbon atom bonded bridge allows the linking of two additional substituents, R_1 and R_2 :

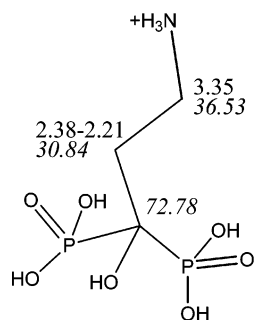


Normally, the R_1 side chain is an alkyl group and the R_2 side chain is a hydroxyl group. Different chemical groups

attached to the second free carbon atom account for the variability in the anti-resorptive potency of the BPs. By increasing the length of the R_1 side chain from a simple methyl to longer alkyl chains, significantly more potent compounds were obtained. Also, amino-bis-phosphonates with amino groups linked to longer alkyl chains are more effective, and the potency reaches the peak when a tertiary nitrogen is included within a ring structure in the R_1 side chain.¹ All the BPs are able to form complexes, both with heavy metal ions and with divalent earth-alkaline metal ions, through the coordination of the phosphonate oxygens.^{2–4} The affinity for metal ions can be further increased if suitable functional groups in the side chains are incorporated. Nitrogen containing BPs showed increased antiresorptive potency.⁵ A great variety of BPs, particularly amino-substituted, are currently available and used in clinical applications. The most common application for these compounds is in osteoporosis, but their use in osteolytic bone diseases, such as Paget's disease and hypercalcemia of malignancy, has rapidly developed.^{6,7} It is known that the BPs strongly bind to hydroxyapatite crystals, preferentially at the sites of increased bone turnover,

* Author to whom correspondence should be addressed. Phone: +39 0577 234388. Fax: +39 0577 234177. E-mail: casolaro@unisi.it.

† Enrolled at the Medical School of Siena University.

Chart 3. ^1H and ^{13}C NMR (in Italics) Chemical Shifts of Pamidronate

columns (G4000 and G3000, from Waters) were used. The running SEC conditions were 0.05 M phosphate buffer + 1 mM EDTA pH 8.75 as a mobile phase, temperature 35 °C, flow rate 0.8 mL/min. The refractive index increment, dn/dc , of both the polymers, with respect to the solvent, was measured by a KMX-16 differential refractometer (from LCD Milton Roy, Riviera Beach, FL). The dn/dc values for oligoPAM and oligoNER were 0.350 and 0.356 mL/g, respectively.

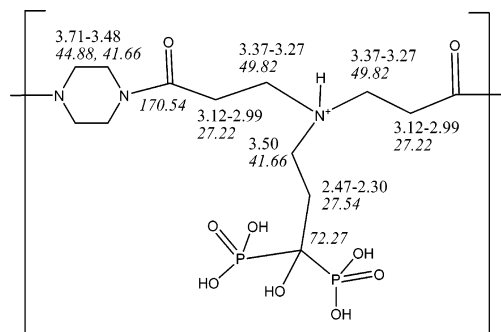
The MALDI-TOF mass spectra were recorded in linear and reflection modes, using a Voyager-DE STR instrument (Perseptive Biosystem) mass spectrometer, equipped with a nitrogen laser ($\lambda = 337$ nm, pulse width = 3 ns), working in a positive ion mode. The accelerating voltage was 25 KV, and the grid voltage and the delay time (delayed extraction, time lag) were optimized for each sample to achieve the higher mass resolution (fwhm). The laser irradiance was maintained slightly above threshold. The samples used for the MALDI analyses were prepared as follows: 10 μL of polymer solution (3–4 mg/mL in H_2O) was mixed with 30 μL of HABA solution (0.1 M in CH_3OH), then 1 μL of each analyte/matrix mixture was spotted on the MALDI sample holder and slowly dried to allow the analyte/matrix cocrystallization. The best MALDI mass spectra were obtained in the reflection mode, with a mass resolution of about 5000 Da.

Syntheses. The pamidronate was prepared according to reported procedures with some modifications.^{24–26}

Synthesis of *N*-Phthaloyl- β -alanine. Phthalic anhydride (2.0 g, 13.5 mmol) was dissolved in acetic acid (10 mL) and treated with β -alanine (1.214 g, 13.5 mmol). The resulting solution was kept under stirring for 15 h and then evaporated to dryness under vacuum. The white residue was recrystallized from hot water, and the white needle-shaped crystals obtained were isolated by filtration of the solution, washed with cold water, and dried under vacuum. Yield = 80% (2.362 g). Anal. Calculated for $\text{C}_{11}\text{H}_9\text{NO}_4$: C, 60.22; H, 4.14; N, 6.38%. Found: C, 60.12; H, 4.14; N, 6.39%. MS m/z : 217.9 (M^- , base); MS m/z : 242.0 (22.99, M^+), (base).

Synthesis of 1-Hydroxy-3-(*N*-phthaloylamino)propylene-1,1-bis-phosphonic Acid. *N*-Phthaloyl- β -alanine (0.50 g, 2.28 mmol) was dissolved in 9.3 mL of SOCl_2 . The resulting solution was heated under reflux for 2 h and then evaporated to dryness under vacuum. The white residue was dissolved in tetrahydrofuran (10 mL) and treated with tris(trimethylsilyl)phosphite (2.28 mL, 6.84 mmol) at 0 °C. The solution was kept under stirring for 5 min at 0 °C and, successively, for 10 min at room temperature. The solution was then treated with CH_3OH (9.3 mL) and kept under stirring for 1 h at room temperature. The solvent and the volatile components were removed under reduced pressure to obtain viscous oil that was treated with diethyl ether (100 mL). The resulting white residue was then isolated by filtration of the solution, washed with diethyl ether, and dried under vacuum. Yield = 90% (0.916 g).

Synthesis of 3-Amino-1-hydroxy-propylene-1,1-bis-phosphonic Acid (Pamidronate). 1-Hydroxy-3-(*N*-phthaloylamino)propylene-1,1-bis-phosphonic acid (0.916 g, 2.52 mmol) was dissolved in 15 mL of concentrated HCl. The resulting solution was heated under reflux overnight. After cooling, the solution was evaporated to dryness under vacuum, and the yellow residue was treated with absolute EtOH at 70

Chart 4. ^1H and ^{13}C NMR (in Italics) Chemical Shifts of oligoPAM

°C for 1 h to take up the phthalic acid. The suspension was hence filtrated, and the white product was washed repeatedly with hot EtOH (70 °C) and then with diethyl ether. The solid was dried under vacuum and recrystallized from water. Yield = 63% (0.373 g).

Anal. Calculated for $\text{C}_3\text{H}_{12}\text{NO}_7\text{P}_2$: C, 15.33; H, 4.72; N, 5.96%. Found: C, 15.66; H, 4.39; N, 6.05%.

^1H NMR (D_2O): 3.35 (t, 2H, $^3J_{\text{H,H}} = 6.95$ Hz), 2.38–2.21 (m, $^3J_{\text{H,H}} = 6.95$ Hz, $^3J_{\text{H,P}} = 13.17$ Hz) ppm. ^{13}C NMR (D_2O) = 72.78 (t, 1C, $^1J_{\text{C,P}} = 127.70$ Hz), 36.53 (t, 1C, $^3J_{\text{C,P}} = 7.69$ Hz), 30.84 (s, 1C) ppm (Chart 3).

^{31}P NMR (D_2O) = 18.97 ppm.

Polyaddition of Pamidronate to 1,4-Bis-acryloylpiperazine (OligoPAM). The oligoPAM was prepared according to a previously reported procedure²⁷ starting from the 1,4-bis(acryloyl)piperazine (BSA: 1.66 g, 0.0085 mol) and a stoichiometric quantity of pamidronate (PAM: 2.00 g, 0.0085 mol) dissolved in twice-distilled water. The solution of PAM (4 mL) containing triethylamine (TEA: 5 mL, 0.0358 mol) was slowly added to the BSA solution (4 mL) under stirring and with an external ice-cooling bath. The mixture was allowed to react for 2 weeks under nitrogen atmosphere at room temperature with occasional stirring. Then, the mixture was run on a column filled with HCl-treated and water-washed Amberlite IRC-50 (25 g) to eliminate the triethylammonium salt. The recovered solution was dried in vacuo. The residue was dissolved in methanol (10 mL) and precipitated in an excess of diethyl ether (600 mL). The white solid was washed twice (300 mL) with fresh ether and dried in vacuo: yield, 2.86 g (78%).

The compound, analyzed by potentiometry, spectroscopy, and elemental analysis, was found to be consistent with the proposed structure.

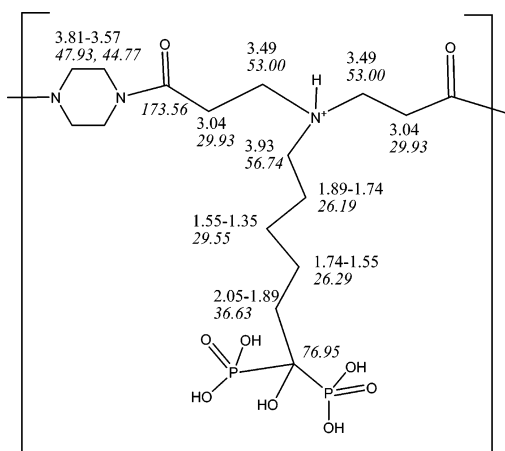
Anal. Calculated for oligoPAM·1/2Et₂O ($\text{C}_{15}\text{H}_{30}\text{N}_3\text{O}_5\text{P}_2$): C, 38.63; H, 6.48; N, 9.01%. Found: C, 37.92; H, 7.21; N, 8.98%.

^1H NMR (D_2O): 3.71–3.48 (m, 8H), 3.50 (br, 2H), 3.37–3.27 (br, 2H), 3.12–2.99 (br, 2H), 2.47–2.30 (br, 2H) ppm. ^{13}C NMR (D_2O) = 170.54, 72.27, 49.82, 44.88, 41.66, 27.54, 27.22 ppm (Chart 4).

^{31}P NMR (D_2O) = 18.43 ppm.

Polyaddition of 6-Amino-1-hydroxyhexylidene-bis-phosphonate (Neridronate) to 1,4-Bis-acryloylpiperazine (OligoNER). The oligoNER was prepared following a procedure similar to that described previously for oligoPAM, by using sodium neridronate (2.00 g, 0.0067 mol), dissolved in twice-distilled water (6 mL) and containing TEA (4 mL, 0.0287 mol), and BSA (1.30 g, 0.0067 mol) dissolved in twice-distilled water (2 mL). The starting milky solution, due to the scarce solubility of the NER, became clear as the reaction proceeded. Yield, 2.85 g (86%). The spectroscopic characterization (^1H NMR, FT-IR) was in line with the proposed structure. Elemental analysis and potentiometric purity were found consistent with a structure comprising three water molecules for each monomer unit. Anal. Calculated for oligoNER·3H₂O ($\text{C}_{16}\text{H}_{38}\text{N}_3\text{O}_{12}\text{P}_2$): C, 36.50; H, 7.28; N, 7.98%. Found: C, 36.14; H, 6.69; N, 7.58%.

^1H NMR (D_2O): 3.81–3.57 (m, 8H), 3.93 (br, 2H), 3.49 (br, 2H), 3.04 (br, 2H), 2.05–1.89 (m, 2H), 1.89–1.74 (m, 2H), 1.74–1.55 (m, 2H), 1.55–1.35 (m, 2H) ppm. ^{13}C NMR (D_2O): 173.56 (s, 1C), 76.95 (t, 1C, $^1J_{\text{C,P}} = 134.86$ Hz), 56.74 (s, 1C), 53.00 (s, 1C), 47.93 (s, 2C),

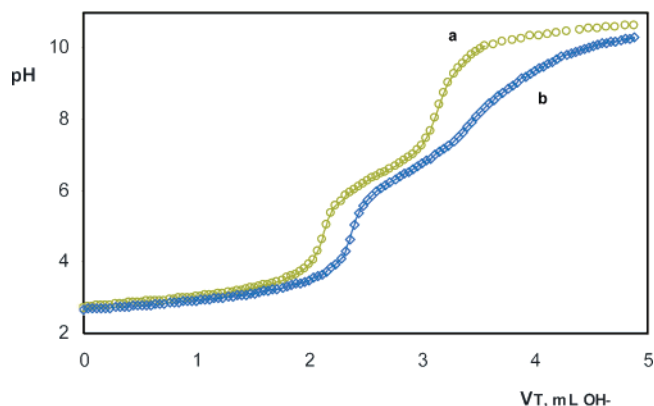
Chart 5. ^1H and ^{13}C NMR (in Italics) Chemical Shifts of oligoNER

44.77 (s, 2C), 36.63 (s, 1C), 29.93 (s, 1C), 29.55 (s, 1C), 26.29 (s, 1C), 26.19 (s, 1C) (Chart 5). ^{31}P NMR (D_2O) = 20.17 ppm.

Potentiometric Measurements. The acid–base potentiometric measurements were performed at 25 °C in aqueous solution (0.15M NaCl) following a previously reported procedure.²⁸ The potentiometric data, E (volt) in relation to V_T (milliliter), were obtained with a TitraLab 90 (from Radiometer Analytical) titration system controlled by TimTalk 9, a Windows-based software. For the titration experiments, a weighed amount of sample (pamidronate: 0.08–0.14 mmol; oligoPAM: 0.07–0.11 mmol; neridronate: 0.11–0.21 mmol; and oligoNER: 0.10–0.11 mmol) was dissolved in 100 mL of 0.15 M NaCl contained in a thermostated glass cell. A measured volume of standard 0.1 M HCl solution was added under magnetic stirring, and a pressurized nitrogen stream was maintained over the surface of the solution to avoid the CO_2 contamination. Stepwise titrations, performed with a standard 0.1 M NaOH solution at different equilibration times (300 and 500 s for each titration step), showed reliable results. The E° calibration was performed before and after each titration by using tris(hydroxymethyl)aminomethane as a standard reagent. The solution pH was calculated through the relation $\text{pH} = (E^\circ - E)/59.16$. Among the considered compounds, only the sodium neridronate solution showed opalescence at $\text{pH} > 10$. Figure 1 shows the titration curve comparison of the neridronate and the corresponding oligomer.

However, in all cases, the purity of the compounds was revealed by end-point analysis. The basicity constants ($\log K_s$) were evaluated with the Superquad program,²⁹ running on PC. At least three replicates were averaged.

Calorimetric Measurements. Solution calorimetric titrations were carried out in the isothermal mode at 25 °C with the model 1250 Tronac calorimeter, as reported elsewhere.²⁸ A weighed amount of BPs (pamidronate, 0.07–0.09 mmol; oligoPAM, 0.05–0.07 mmol; neridronate, 0.09–0.10 mmol; and oligoNER, 0.06–0.08 mmol) and a measured volume of standard 0.1 M NaOH solution were dissolved in 25 mL of aqueous 0.15 M NaCl in a stainless steel reaction vessel. The amount of the latter solution was controlled to have only a partial or a complete deprotonation of the BPs acid sites. In the case of neridronate, the amount of the added NaOH was limited to the deprotonation of the phosphonate oxygens only. A standardized 0.1 M HCl solution was used as a titrant and delivered through a Gilmont buret at the Buret Delivery Rate (BDR) of 0.0833 mL/min. The chemical calibration with the standard reagent tris(hydroxymethyl)aminomethane, as well as the corrections for the titrant heats of dilution, was made before and after each titration run. All the measurements were automatically controlled by the Thermal program (from Tronac Inc.), which was configured to operate through a NI-DAQ (National Instruments) driver software in Windows. The graphical programming language LabView was used to create the application. The enthalpy change values were evaluated with the Fith program,³⁰ while the entropy

**Figure 1.** Potentiometric titration curves of neridronate (a) and corresponding oligoNER (b) in 0.15 M NaCl at 25 °C.

changes were calculated by the Gibbs–Helmholtz equation. At least three replicates were averaged, and the standard deviation was calculated.

Viscometric Measurements. Viscometric titration data were obtained at 25 °C in an aqueous solution by using an automatic Schott-Gerate viscometer (AVS 310). A weighed amount of oligomer (oligoPAM, 0.0800 mmol and oligoNER, 0.0703 mmol) was dissolved in 25 mL of 0.15 M NaCl containing a measured quantity of standard 0.1 M HCl solution. A standardized 0.1 M NaOH solution was stepwise delivered by a Metrohm Multidosimat piston buret. The pH value at each neutralization step was evaluated with the Fith program³⁰ by using the previously evaluated $\log K_s$.

Toxicity Tests. The cell viability was evaluated by using a Cell Counting Kit (WST-1 method³¹ Dojindo Lab., Tokyo, Japan). Briefly, after the MC3T3-E1 cells (Japan Riken Cell Collection) reached confluency, they were trypsinized, seeded at 1×10^4 cells/cm² onto a 96-well multiplate (Corning), and incubated for 2 days at 37 °C in a humidified atmosphere containing 5% CO_2 . After removal of the culture medium, 100 mL of a bis-phosphonate solution (or suspension) in fresh culture medium supplemented with 10% (v/v) FBS (pH 7.2) was added to each well and allowed to stand for at 37 °C in a fully humidified atmosphere with a volume fraction of 5% CO_2 . The bis-phosphonate concentration of oligoPAM and oligoNER is referred to as the monomer unit of the oligomers. After 24 h incubation, 10 mL of WST-1 reagent was added to the wells, which were incubated for a further 2 h at 37 °C. A total of 10 mL of 0.1 N HCl aqueous solution was then added to each well to stop the reaction. To remove insoluble bis-phosphonate samples, the plate was centrifuged (1000 rpm, 5 min), and then 50 mL of supernatant was transferred to another plate. The absorbance of the aliquot of the solution was measured at 450 nm with a multiplate reader (Bio-Rad model 650, Tokyo, Japan), taking as reference the absorbance at 655 nm. The results were expressed as viability (%) related to a control untreated with the test samples. The error bar means standard error relative to four experiments.

Biological Effects on Primary Human Osteoblastic Cells. Bone Samples. Bone samples were obtained from four women and men (aged 56–78 years, with a mean age of 66 years) who underwent total hip replacement surgery for degenerative joint disease. The patients were selected excluding those who had sex steroid deficiency or had received a previous therapy with bis-phosphonates, hormone replacement, or GC treatment during the previous 2 years. The experiments were conducted using cells from individual patients, and the specimens were not pooled. First-passage human osteoblastic cells (hOB) from primary cultures of trabecular bone explants were used.

Cell Cultures. Fragments of trabecular bone were washed extensively in PBS to remove blood and bone marrow and then explanted into culture in Dulbecco's modified Eagle's Medium (DMEM) (Gibco, Life Technologies) supplemented with 10% FCS (Sigma), and 2 mM L-glutamine (Gibco, Life Technologies). The cultures were incubated at 37 °C in a humidified atmosphere of 7% $\text{CO}_2/93\%$ air.³² The cells

were maintained by removing the conditioned medium and replacing it with fresh DMEM supplemented with 10% FCS every 7 days. After 3–6 weeks in culture, a cellular confluent monolayer had grown out from the bone fragments. The primary cell layers (E1) were washed in PBS and then treated for 5 min with a 0.05% trypsin/0.02% EDTA solution (Gibco, Life Technologies). The detached cells were passed at a density of 60,000 cell/well into a 12-well multiplate (Corning Costar Corp.) and cultured in DMEM with 10% FCS until the confluence (E1P1). The medium was changed twice a week, and after this period, the cells were washed in PBS and incubated for further 48 h with serum-free medium supplemented with 0.1% BSA (Sigma). During the drug treatment, each culture medium was changed twice a week, adding 1 mL of DMEM with 10% FCS containing different concentrations of simple (PAM and NER) and oligomeric (oligoPAM and oligoNER) drugs. The effect of each drug concentration was tested in triplicate for each different cell culture.

Proliferation Assay. The proliferative response of the osteoblast cells to different NER, PAM, oligoNER, and oligoPAM concentrations (10^{-13} to 10^{-8} M) was examined by a colorimetric assay system based on tetrazolium salt reduction (MTT, Boehringer Mannheim, Germany). Briefly, each hOB culture was incubated with 0.5 mg/mL of the 3-(4,5-dimethylthiazol-2-yl)-2,5-diphenyl-tetrazolium bromide labeling reagent for 4 h in a humidified atmosphere. The resultant purple formazan salt crystals were solubilized with sodium dodecyl sulfate (SDS) in 10 mM HCl. After 1 h of incubation, the solubilized formazan product was spectrophotometrically quantified. The total metabolic activity increased in the sample: it was an evaluation of the increase in the number of living cells. This rise was directly correlated to the amount of purple formazan crystals formed, as monitored by the absorbance.

Biochemical ALKP Assay. The alkaline phosphatase (ALKP) activity was directly measured on the monolayer cultures. The medium was removed, and the cells were washed three times with PBS and shaken for 30 min at 37 °C in 1 mL of 10 mM *p*-nitrophenylphosphate (Sigma). The *p*-nitrophenylphosphate solution was removed, and the reaction was stopped by adding 1 mL of 1 N NaOH. The optical density was measured at 405 nm. The ALKP activity values were normalized to the relative number of viable cells as determined in 12-well plates using the previously mentioned proliferation assay.

Results and Discussion

Synthesis and Characterization. To prepare the two oligomers (oligoPAM and oligoNER), a procedure similar to the Michael-type synthetic pathway to obtain classical poly(amido-amine)s, PAAs, was followed.¹⁴ In the case of ampholyte compounds, triethylamine was used to free the zwitterionic species of the amino-bis-phosphonate (BPs), and this allowed polyaddition to the bisacrylamide, even if the reaction was expected to become extremely sluggish.³³ In fact, in both cases, we obtained oligomeric products with molecular weights lower than that of the amphoteric PAAs previously reported.^{13,20} This may have the advantage of cytosolic access and to be pharmacologically competitive with the BPs action toward the bone resorption cells.

The differential and cumulative molecular weight distributions of the oligoPAM and the oligoNER are reported in Figure 2, showing a quite resolved presence of low molecular weight oligomeric species. However, a rather similar behavior was found in both cases. The main results of their molecular characterization are summarized in Table 1. Here, the weight-average molecular weight M_w is reported along with a meaningful low polydispersity index $D = M_w/M_n$ (M_n is the number-average molecular weight). The molar mass distribution of the two samples was relatively narrow.

The relative low molecular weights and the close D values were probably influenced by the BPs comonomer, strongly

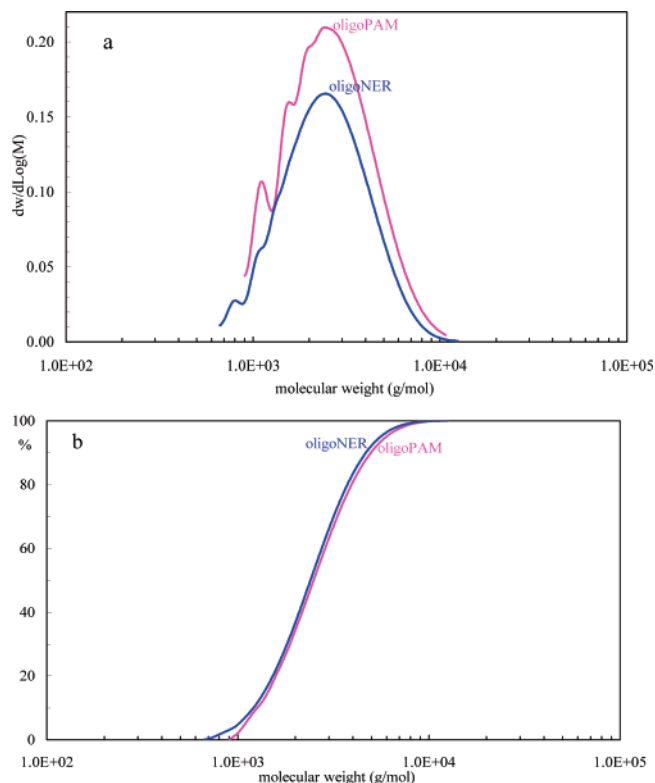


Figure 2. Differential (a) and cumulative (b) molecular weight distributions of oligoPAM and oligoNER.

modifying the physicochemical properties of the oligomer. In fact, in both cases, the dn/dc values were found to be unusually higher than that shown by the PAAs previously reported.¹³

The presence of oligomeric species was confirmed also by MALDI-TOF spectroscopy. The MALDI-TOF spectra of the oligoPAM and the oligoNER are reported in Figure 3, showing peak clusters regularly distributed and falling, respectively, at 429.4 and 471.4 amu, corresponding to the molecular weight of the repeating units of oligoPAM and oligoNER, respectively. The MALDI spectral quality was good for both the samples since the masses were very low, in fact, well-resolved and calibrated mass peaks from 700 up to 3000 Da are observed in Figure 3.

The structure of the oligomers corresponding to the homologous families of peaks in Figure 3 are depicted in Table 2.

In both the spectra, the most intense peaks correspond to the protonated oligomers terminated with unsaturated acryloylpiperazine groups at both the ends (species C in Figure 3 and in Table 2). Ions belonging to the mono- and di-sodium salts of these oligomers were also observed. These families of peaks are accompanied with intense peaks with a mass difference of 101 Da, corresponding to the triethylammonium salts of these oligomers (species D in Figure 3 and in Table 2) that may be formed owing to the low amount of the triethylamine present as an impurity. This result was also confirmed by ¹H NMR that reveals traces of triethylamine in the oligoPAM (0.7 mol %) and oligoNER (0.45 mol %) samples. The mass spectra show also other families of intense peaks due to the protonated and sodium-salified forms of the oligomers terminated with acryloylpiperazine at one side and with an amine unit at the other one (species A in Figure 3 and in Table 2). As well as oligomers of type C, peaks due to the triethylammonium salts of these oligomers were also observed (mass series B in Figure 3 and in Table 2). Weak mass peaks assigned to the oligomers terminated with acryloyl and piperazine moieties (species E)

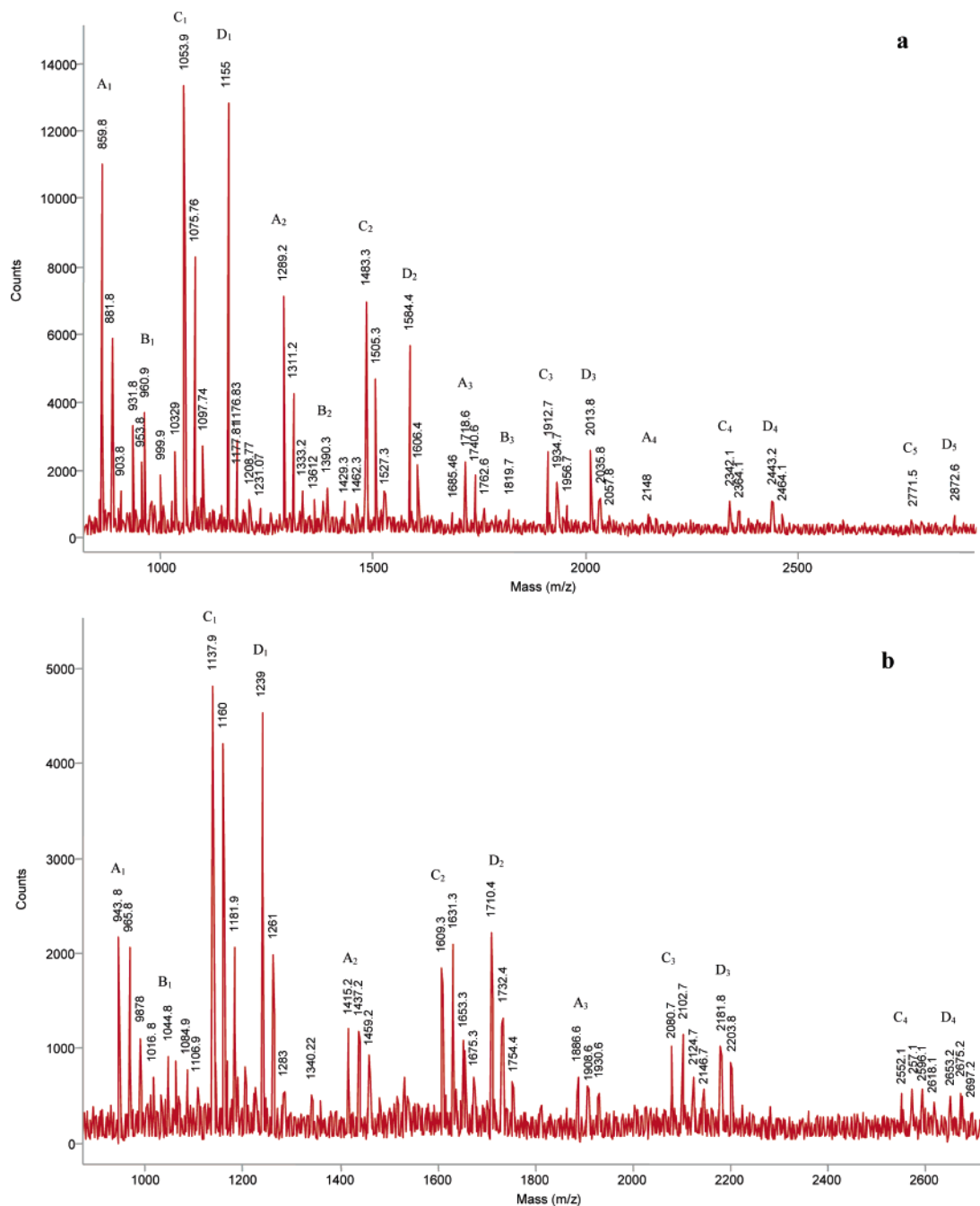


Figure 3. MALDI-TOF spectra of oligoPAM (a) and oligoNER (b).

Table 1. Molecular Characterization Data Obtained from SEC Analysis

compd	M_w (g/mol)	$D = M_w/M_n$
oligoPAM	2880	1.3
oligoNER	2740	1.3

and with acryloyl and acrylic acid end groups (species F) were also present in the MALDI spectra of the samples investigated. Their presence indicates that the hydrolysis reaction might occur during the syntheses of the PAA samples. The sodiated salts of the analyzed oligomers were formed during the preparation of the matrix/analyte mixture for MALDI analysis.

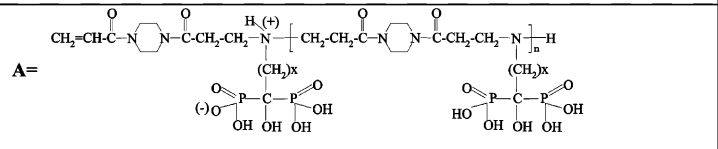
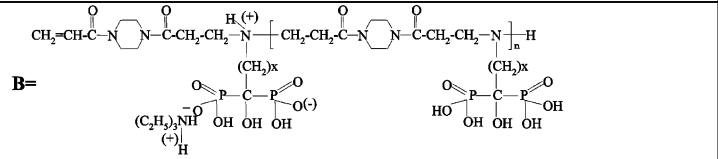
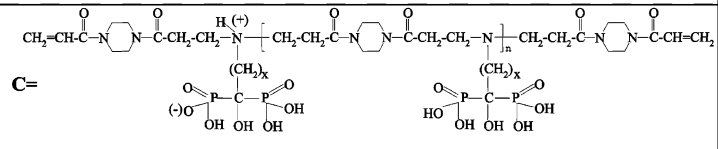
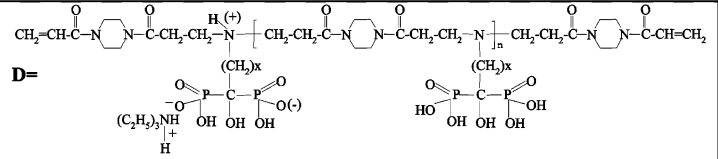
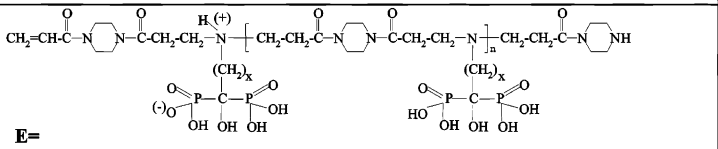
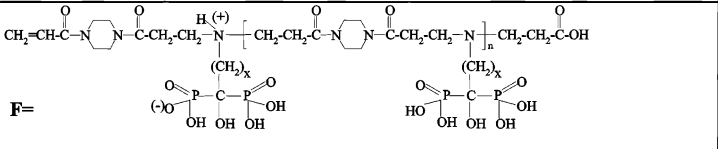
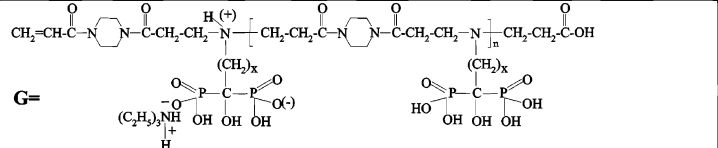
Both the FT-IR and the NMR (^1H , ^{13}C , and ^{31}P) spectroscopies supported the proposed structure. While the infrared frequencies of the oligoPAM were found close to those of the oligoNER, the comparison with the corresponding low molecular weight analogues showed a substantial difference. Table 3

summarizes the observed main IR frequencies in the most significant wavenumber range considered ($800\text{--}1800\text{ cm}^{-1}$). Both the oligomers clearly showed the amide I and amide III frequencies, together with the frequency belonging to the piperazine ring. The phosphoryl $\text{P}=\text{O}$ frequency was also clearly evident in all cases.³⁴

With the exception of the NER that was in the sodium salt form, the potentiometric titrations revealed that PAM was in the completely protonated form, while both the oligomers were somewhat partially protonated or in the zwitterionic forms, due to the higher acidity of two $\text{P}\text{--}\text{OH}$ groups. These different protonation states are reflected also in the ^{31}P NMR signal, in fact, the ^{31}P chemical shift is dependent by the extent of neutralization and hence by the pH.³⁵

Protonation Thermodynamics. The acid–base properties of the two oligomers and of the corresponding low molecular

Table 2. Structural Assignments of Peaks Displayed in the MalDI-TOF Mass Spectra of the OligoPAM and of the OligoNER Samples Reported in Figure 3

Structures ^a	(n)	MH ⁺		(M-H+Na) ⁺		(M-2H+2Na) ⁺	
		X=2	X=5	X=2	X=5	X=2	X=5
A= 	1	859.8	943.8	881.8	965.8	903.8	987.8
	2	1289.2	1415.2	1311.2	1437.2	1333.2	1459.2
	3	1718.6	1886.6	1740.6	1908.6	1762.6	1930.6
	4	2148		2170		2192	
B= 	1	960.9	1044.8	982.9	1066.8		
	2	1390.3	1516.2	1412.3	1538.2		
	3	1819.7		1841.7			
C= 	1	1053.9	1137.9	1075.9	1159.9	1097.9	1181.9
	2	1483.3	1609.3	1505.3	1631.3	1527.3	1653.3
	3	1912.7	2080.7	1934.7	2102.7	1956.7	2124.7
	4	2342.1	2552.1	2364.1	2574.1	2386.1	2596.1
	5	2771.5					
D= 	1	1155	1239	1177	1261		1283
	2	1584.4	1710.4	1606.4	1732.4		1754.4
	3	2013.8	2181.8	2035.8	2203.8		2225.8
	4	2443.2	2653.2	2465.2	2675.2		2694.2
	5	2872.6		2894.6			
E= 	1	999.9	1084.9		1106.9		
	2	1429.3					
F= 	1	931.8	1016.8	953.8	1038.8		
	2	1361.2		1383.2			
	3	1790.6		1812.6			
G= 	1	1032.9					
	2	1462.3					

^a X = 2 corresponds to the oligoPAM samples, whereas X = 5 corresponds to the oligoNER sample.

weight analogues were studied in aqueous 0.15 M NaCl at 25 °C by potentiometry, solution calorimetry, and viscometry.

Table 4 summarizes the thermodynamic functions: basicity constants ($\log K_s$), enthalpy ($-\Delta H^\circ$), and entropy (ΔS°) changes, relative to the four protonation steps that were detectable in these experimental conditions.

Unlike the NER, which showed insolubility at pH > 10, all the other compounds revealed two great $\log K_s$ at high pH values and only a small one at low pH. In all cases, a buffered region separating two sharp end-points allowed the evaluation of an intermediate $\log K$ value, along with the purity of the compound. Both the oligomers showed real basicity constants (i.e., their $\log K_s$ were independent of the degree of protonation of the whole macromolecule, thus behaving as small molecules).³⁶ As a matter of fact, the poly(amido-amine)s, PAAs, are polyelectrolytes whose monomer units behave independently from each other toward protonation and complex formation with metal ions.³⁷ Moreover, although in some ampholyte PAAs the $\log K_s$ are on the borderline between real and apparent, in the present

case, the oligomers are really short macromolecular chains with only a few linked monomer units, behaving thus as many simple oligopeptides.³⁸ In the assignments of $\log K$ to the corresponding basic group being protonated, some difficulties that may arise²⁻⁴ will be overcome by the help of the enthalpy and entropy change values. These thermodynamic functions allow us to hypothesize a protonation-like mechanism. The first protonation step of the fully ionized PAM will be relative to the basic nitrogen, as also occurs in the corresponding oligoPAM. This protonation leads to the formation of a clustered zwitterionic species where the ionized oxygens forms H-bonded structures toward the onium ion, involving two seven-membered rings condensed with a six-membered one of the bis-phosphonate moiety in the PAM. In the corresponding oligomer, the two additional amido-oxygens may further on contribute, with a six-chelate ring, to a more compact structure (Chart 6), as also evidenced in previously studied poly(amido-amine)s.^{20,39}

This hypothesis is well-supported by the very large $-\Delta H^\circ$ value and the corresponding very low ΔS° . OligoPAM showed

Table 3. Observed Infrared Frequencies (cm^{-1}) for the Amino-bis-phosphonate Compounds^a

PAM	oligoPAM	NER	oligoNER
1646 m		1636 s	
	1632 vs amide I		1632 vs amide I
1627 s			
1547 s		1539 s	
1473 w	1473 s	1473 m	1473 s
1446 w	1446 s	1446 w	1446 s
1397 s	1393 m		
	1365 w		1368 m
1301 m			
	1284 s amide III		1283 s amide III
	1246 s	1242 sh	1242 s
1228 m	1224 s	1220 sh	1221 s
1166 m	1159 vs P=O stretching	1159 vs	1163 vs P=O stretching
1126 s	1126 sh		
1091 m	1057 vs	1050 vs	1052 vs
	1021 vs piperazine ring		1016 vs piperazine ring
991 vs	991 w		981 m
936 vs			
920 sh	911 s	905 vs	909 vs
836 m	842 m		

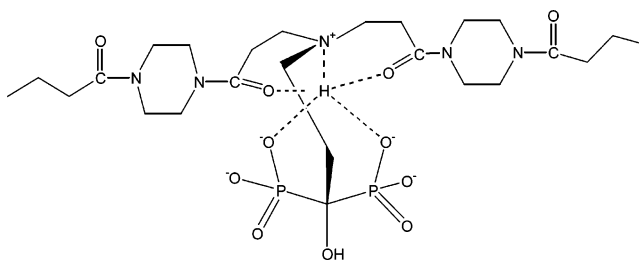
^a vs: Very strong; s: strong; m: medium; w: weak; and sh: shoulder.

Table 4. Thermodynamic Functions of Simple and Oligomeric Amino-bis-phosphonate Protonation at 25 °C in 0.15 M NaCl

protonation step	log <i>K</i>	$-\Delta G^\circ$ (kJ/mol)	$-\Delta H^\circ$ (kJ/mol)	ΔS° (J/mol K)
PAM				
first	11.02 (1)	62.91 (6)	64.4 (2.9)	-5 (9)
second	9.90 (1)	56.51 (6)	16.7 (2.9)	133 (9)
third	5.86 (1)	33.45 (6)	4.6 (4)	97 (1)
fourth	2.04 (2)	11.64 (11)	-4.2 (4)	53 (2)
OligoPAM				
first	9.95 (3)	56.80 (17)	55.7 (7)	4 (3)
second	9.55 (2)	54.52 (11)	19.3 (2.9)	118 (10)
third	5.94 (3)	33.91 (17)	6.7 (3)	91 (2)
fourth	2.10 (9)	12.0 (5)	-3.2 (1.1)	51 (5)
NER				
first	<i>a</i>	<i>a</i>	<i>a</i>	<i>a</i>
second	10.66 (3)	60.85 (17)	44.5 (3)	55 (2)
third	6.50 (3)	37.10 (17)	3.4 (4)	113 (2)
fourth	2.45 (4)	13.98 (23)	-5.1 (7)	64 (3)
OligoNER				
first	10.88 (2)	62.11 (11)	42.6 (3)	65 (2)
second	9.20 (2)	52.52 (11)	35.2 (1.5)	58 (5)
third	6.51 (2)	37.16 (11)	4.4 (2)	110 (1)
fourth	2.37 (3)	13.53 (17)	-8.5 (4)	74 (2)

^a Not detectable for insolubility of the species. The values in parentheses are standard deviations.

lower basicity, even if greater than expected, and the lower enthalpy contribution being the basic nitrogen tertiary in nature.⁴⁰ The log *K* of 9.95 found for oligoPAM (Table 4) is in line with the previously hypothesized mechanism, which was further corroborated by the viscometric measurements. In fact, the protonation of the basic nitrogen strongly reduced the coil of the oligoPAM, in spite of many negative free charges present on the macromolecule at high pHs. Figure 4 shows the reduced viscosity values of oligoPAM at different pHs, along with the superimposing distribution curves.

Chart 6. Structure of the Nitrogen-Protonated oligoPAM

By lowering the pH, a flat viscosity trend was consistent with the protonation of a more basic phosphonate oxygen. The protonation process decreased the negative charge in a wide pH range, including the physiologic one. In the meantime, the breaking of the H-bond led to a larger ΔS° and a lower $-\Delta H^\circ$ value. The protonation of the further two phosphonate oxygens, at the lower pH values, correspondingly reduced the macromolecular coil because of the decrease in electrostaticity and increased the ΔS° value for the larger freedom of the bis-phosphonate moiety and the greater release of structured water molecules.

On the other hand, oligoNER showed a quite different protonation mechanism. The longer methylene chains render less soluble NER in the free form, even if many negative charges are present on one side. The presence of the two additional amido groups in the corresponding oligomer improves the solubility, even at high pHs. In the oligoNER, the first and greater log *K* was assigned to the phosphate oxygen because of the similarity with the free NER. The greater value of log *K* may be attributed to higher electrostatic effects exerted by the more negatively charged oligoNER. The tertiary nitrogen is protonated as a second step, and this does not allow a compactness in the structure. The $-\Delta H^\circ$ value of 35.2 kJ/mol (Table 4) lies in the range of the tertiary nitrogen protonation, as well as the fact that the entropy contribution does not indicate a tidy structure, and the flatter viscometric data showed the major role played by the negative charges. In fact, only at low pH, when the zwitterionic LH_4^\pm (L^{4-} is the monomer unit in the completely ionized form) species is prevailing, the reduced viscosity drops to negligible values as a consequence of a compact coil conformation. The further two protonation steps, involving the phosphate oxygens, showed closer thermodynamic functions for both the oligoNER and the corresponding simple NER.

Biological Effects on Animal and Human Osteoblasts. It is well-known that the osteoblastic cells aid growth and development of bones. On the other hand, the osteoclast cells actively reabsorb old or fatigued bone so that new bone may be replaced by osteoblast cells. When osteoclast cells reabsorb bone faster than the osteoblast cells are building it, then bone loss (osteoporosis) occurs.⁴¹

Although the most important biological effect of BPs is the reduction of the bone remodeling through the direct inhibition of the osteoclast activity, there is a lot of experimental evidence that is in concordance with the hypothesis that an alternative cellular target of BPs is represented by the osteoblasts. Several studies have been performed to assess the effect of BPs on human osteoblastic cells. Recent data suggest that BPs can transiently stimulate the proliferation and increase the differentiation of human osteoblasts to different extents, depending on the compounds tested.^{42,43} Thus, there is an increasing amount of experimental data that suggest that these pharmacological compounds exert their inhibitory effect on the osteoclast

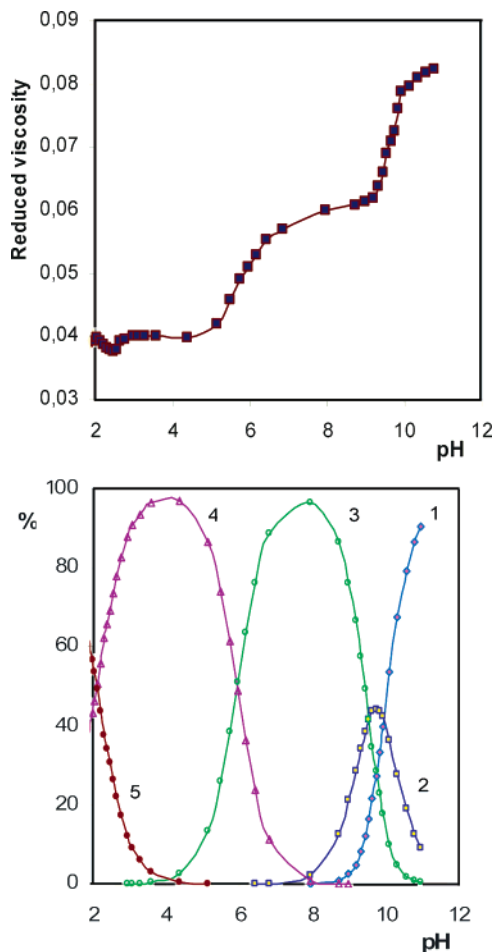


Figure 4. Reduced viscosity (η/C , dL/g) and species distribution curves (%) in relation to pH of oligoPAM at 25 °C in 0.15 M NaCl. (Ligand protonation form: 1, completely ionized; 2, nitrogen mono-protonated; 3, diprotonated; 4, triprotonated; and 5, tetraprotonated.)

functions both directly and indirectly through a metabolic action on the osteoblasts.

To demonstrate if our new synthesized oligoBPs possess pharmacological features comparable to those observed for their corresponding low molecular weight analogues, we investigated in vitro their biological effects on osteoblastic cells of animal or human origins.

A first series of experiments (citotoxicity tests) were performed on osteoblasts derived from a murine cell line (MC3T3-E1) generally used as reference in this kind of experiments. The cell cultures were treated for 24 h with very high concentrations of the drugs (10^{-5} to 10^{-3} M). These concentrations are up to 3 orders of magnitude higher than the therapeutic dose⁴³ but are retained to be transiently reached at the level of the resorption lacunae during the bone remodeling. As reported in Figure 5, the proliferation of the osteoblastic cells in the presence of oligoBPs is comparable, and in some cases, it is enhanced to that shown by the commercial drugs used in clinical practice.

A similar series of experiments was then performed on human osteoblasts using a wide range of BPs and oligoBPs concentrations for prolonged periods of time. Our results demonstrate that both the simple and the oligomeric forms of NER and PAM can slightly modify the proliferation activity of human osteoblasts in vitro. Figures 6 and 7 show a comparison between the cell proliferations after 48 h and 96 h, in the presence or absence of different concentrations of NER and oligoNER (Figure 6) or PAM and oligoPAM (Figure 7).

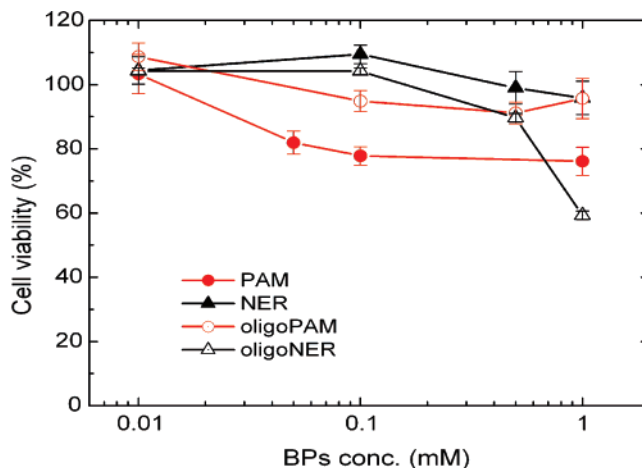


Figure 5. Cytotoxicity of oligomers and corresponding amino-bis(phosphonate) analogues against mouse osteoblasts (MC3T3-E1).

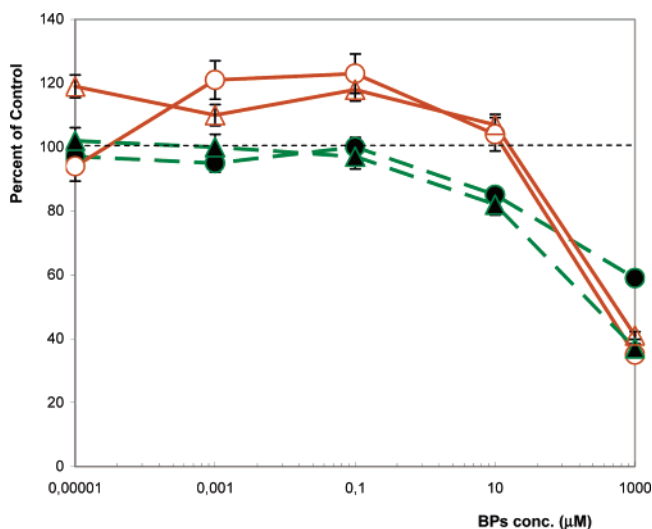


Figure 6. Effects of different NER (circle) and oligoNER (triangle) concentrations on human osteoblast proliferation after 48 h (dotted lines) and 96 h (solid lines).

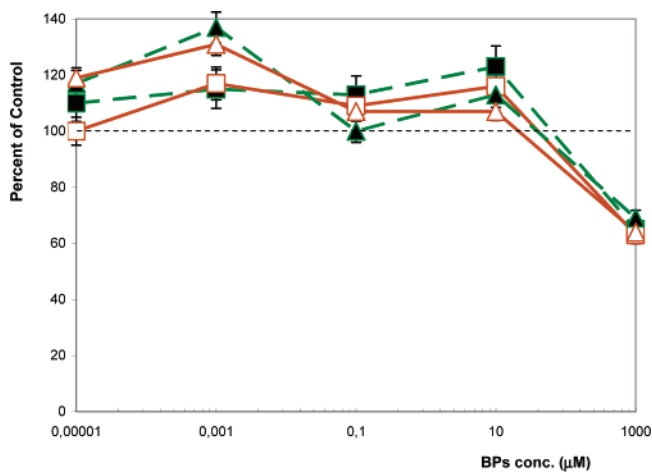


Figure 7. Effects of different PAM (square) and oligoPAM (triangle) concentrations on human osteoblasts proliferation after 48 h (dotted lines) and 96 h (solid lines).

A significant increase of the cell proliferation (about +20%) was observed for NER and oligoNER after 96 h of treatment. In comparison with NER, the oligoNER seems to be effective also at lower concentrations (less than 10^{-9} M). The PAM is able to induce a slight increase of the cell proliferation (up to +16%)

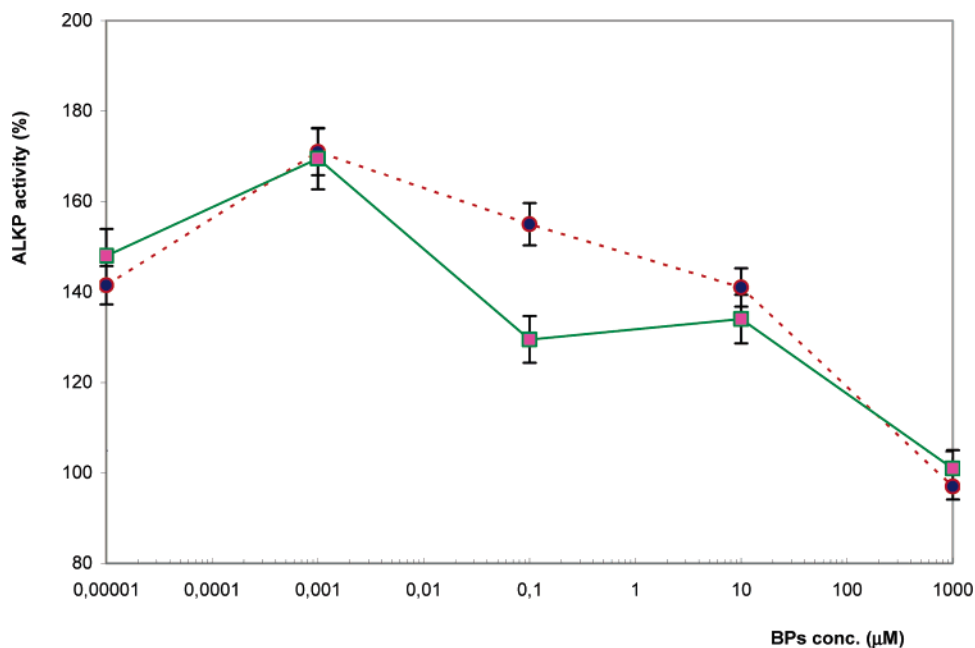


Figure 8. Effect of NER (dotted line) and oligoNER (solid line) concentrations on alkaline phosphatase activity in human osteoblasts.

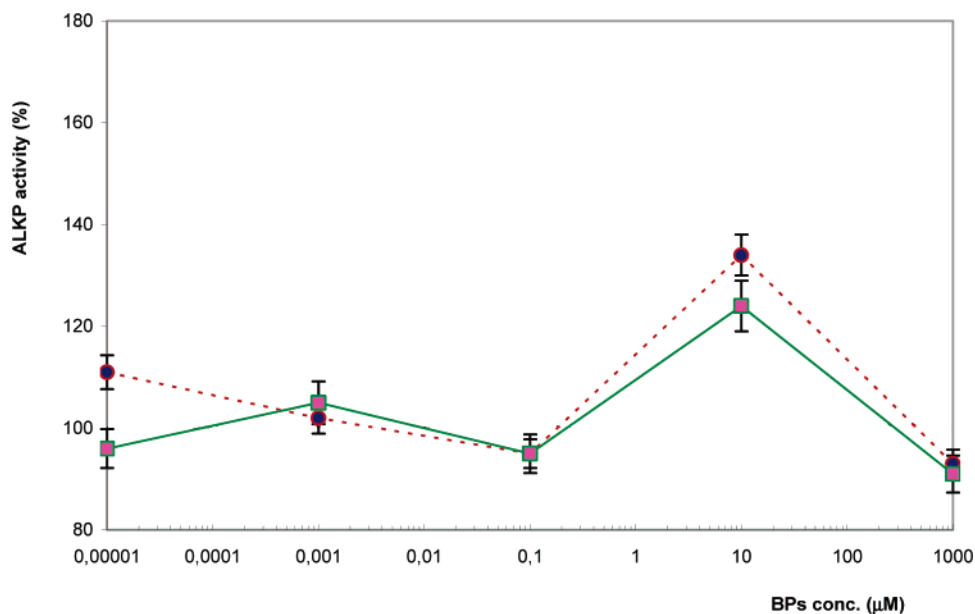


Figure 9. Effect of PAM (dotted line) and oligoPAM (solid line) concentrations on alkaline phosphatase activity in human osteoblasts.

at concentrations in the range of 10^{-5} M, whereas the oligoPAM seems to induce a maximum of proliferation (+31%) after 96 h at concentrations surrounding 10^{-9} M. These results seem to be encouraging because the oligomers do not have any negative effect on the cellular metabolism at the drug concentration lower than the therapeutic dose.

Effects on Osteoblast Activity. To assess whether oligoBPs affect the osteoblast differentiation, we evaluated the ALKP activity, a classical osteoblastic marker. ALKP is released by osteogenic precursor cells as an early sign of osteoblastic differentiation in culture. In our study, after 7 days, all the tested BPs and oligoBPs induced a bell-shaped response of ALKP activity (Figures 8 and 9). The NER and the oligoNER induced a potent stimulation of the ALKP activity (up to +72%) at concentrations surrounding 10^{-9} M (Figure 8). On the contrary, the PAM and the oligoPAM induced a milder stimulation of the ALKP activity (max +37%) at drug concentrations surrounding 10^{-5} M (Figure 9).

Conclusion

The paper, concerned with the synthesis and characterization of novel therapeutic compounds with amino-bis-phosphonate residues, is a further development of the poly(amido-amine) chemistry containing comonomers of biological interest.⁴⁴ We reported the protonation thermodynamics of two oligomers containing BP residues of different chain lengths (pamidronate and neridronate) that seem to be an important factor in potency.⁴⁵ The different thermodynamic data showed a different protonation mechanism. Unlike the oligoNER, with a longer residual aliphatic chain, the oligoPAM showed a high compactness when the tertiary basic nitrogen was protonated. The structure involved both the side chain phosphonate oxygens and the carbonyl oxygens in the main chain. The reduced coil dimensions make the oligomer more suitable for cytosolic access. The suitable short macromolecular chains of low polydispersity index and the ability to degrade at physiological conditions make these

kinds of oligomers good candidates to be used in long-term therapy for bone resorption.⁴¹ Both the animal and the human osteoblasts underwent a remarkable low toxicity effect at high as well as at low concentrations of the BPs. At therapeutic doses, both the oligomers showed human osteoblast proliferation close to that shown by the corresponding simple drug precursor. Moreover, the use of oligomeric compounds may overcome the observed usual poor absorption of the BPs.⁴¹ The absorption of BPs may be increased by purposely designing oligomers of suitable lipophilicity, which enhances transcellular transport across the epithelial barriers.

Studies are in progress for the evaluation of the metal complex ability toward calcium ions to find oligomers with more potent antiresorptive activity that gives a broad safety margin for normal mineralization.

Acknowledgment. The work was partially supported by a grant of the MIUR (Rome, Italy), as a project within PRIN2004, and by a grant of Siena University (PAR2005). Thanks are due to Dr. S. Rosini (Director R&D Division of Abiogen Pharma SpA, Pisa, Italy) for providing a free sample of pure research sodium neridronate.

References and Notes

- Santini, D.; Vespasiani Gentilucci, U.; Vincenti, B.; Picardi, A.; Vasaturo, F.; La Cesa, A.; Onori, N.; Scarpa, S.; Tonini, G. *Ann. Oncol.* **2003**, *14*, 1468.
- Irani, R. R.; Moedritzer, K. *J. Phys. Chem.* **1962**, *66*, 1349.
- Zeevaart, J. R.; Jarvis, N. V.; Louw, W. K. A.; Jackson, G. E.; Cukrowski, I.; Mouton, C. J. *J. Inorg. Biochem.* **1999**, *73*, 265.
- Zeevaart, J. R.; Jarvis, N. V.; Louw, W. K. A.; Jackson, G. E. *J. Inorg. Biochem.* **2001**, *83*, 57.
- Jung, A.; Bisaz, S.; Fleish, H. *Calcif. Tissue Res.* **1973**, *11*, 269.
- Hardman, J. G.; Limbird, L. E.; Molinoff, P. B.; Ruddon, R. W. In *The Pharmacological Basis of Therapeutics*; McGraw-Hill: NY, 1995.
- Miller, P. D.; Brown, J. P.; Siris, E. S. *Am. J. Med.* **1999**, *106*, 513.
- Herczegh, P.; Buxton, T. B.; McPherson, J. C.; Kovács-Kulyassa, A.; Brewer, P. D.; Sztaricskai, F.; Stroebel, G. G.; Plowman, K. N.; Farcasiu, D.; Hartmann, J. F. *J. Med. Chem.* **2002**, *45*, 2338.
- Vachal, P.; Hale, J. J.; Lu, Z.; Streckfuss, E. C.; Mills, S. G.; MacCoss, M.; Yin, D. H.; Algayar, K.; Manser, K.; Kesisoglou, F.; Ghosh, S.; Alani, L. L. *J. Med. Chem.* **2006**, *49*, 3060.
- Bansal, G.; Wright, J. E. I.; Kucharski, C.; Uludag, H. *Angew. Chem., Int. Ed.* **2005**, *44*, 3710.
- Wang, L.; Zhang, M.; Yang, Z.; Xu, B. *Chem. Commun.* **2006**, 2795.
- Heymann, D.; Ory, B.; Gouin, F.; Green, J. R.; Rédini, F. *Trends Mol. Med.* **2004**, *10*, 337.
- Ferruti, P.; Manzoni, S.; Richardson, S. C. W.; Duncan, R.; Patrick, N. G.; Mendichi, R.; Casolaro, M. *Macromolecules* **2000**, *33*, 7793.
- Ferruti, P. In *Polymeric Materials Encyclopedia*; Salamone, J. C., Ed.; CRC Press Inc.: Boca Raton, FL; 1996; Vol. 5, p 3334.
- Richardson, S.; Ferruti, P.; Duncan, R. *J. Drug Targeting* **1999**, *6*, 391.
- Ranucci, E.; Spagnoli, G.; Ferruti, P.; Sgouras, D.; Duncan, R. *J. Biomater. Sci., Polym. Ed.* **1991**, *2*, 303.
- Ferruti, P.; Marchisio, M. A.; and Duncan, R. *Macromol. Rapid Commun.* **2002**, *23*, 332.
- Duncan, R. *Nat. Rev.* **2003**, *2*, 347.
- Patrick, N. G.; Richardson, S. C. W.; Casolaro, M.; Ferruti, P.; Duncan, R. *J. Controlled Release* **2001**, *77*, 225.
- Malgesini, B.; Ferruti, P.; Manfredi, A.; Casolaro, M.; Chiellini, F. *J. Bioact. Compat. Polym.* **2005**, *20*, 377.
- Montaudo, G.; Montaudo, M. S.; Samperi, F. In *Mass Spectrometry of Polymers*; Montaudo, G., Lattimer, R. P., Eds.; CRC Press: Boca Raton, FL, 2002; Chs. 2 and 10.
- Montaudo, G.; Samperi, F.; Montaudo, M. S. *Prog. Polym. Sci.* **2006**, *31*, 277.
- Mendichi, R.; Giacometti Schieron, A. In *Current Trends in Polymer Science*; Pandalai S. G., Ed.; Trans-World Research Network: Trivandrum, India, 2001; Vol. 6, p 17.
- Krauser, S. F.; Watterson, A. C. *J. Org. Chem.* **1978**, *43*, 2026.
- Griffiths, D. V.; Hughes, J. M.; Brown, J. W.; Caesar, J. C.; Swetnam, S. P.; Cumming, S. A.; Kelly, J. D. *Tetrahedron* **1997**, *52*, 17815.
- Lecouvey, M.; Mallard, I.; Bailly, T.; Burgada, R.; Leroux, Y. *Tetrahedron Lett.* **2001**, *42*, 8475.
- Barbucci, R.; Casolaro, M.; Nocentini, M.; Corezzi, S.; Ferruti, P.; Barone, V. *Macromolecules* **1986**, *19*, 37.
- Casolaro, M.; Bottari, S.; Cappelli, A.; Mendichi, R.; Ito, Y. *Biomacromolecules* **2004**, *5*, 1325.
- Gans, P.; Sabatini, A.; Vacca, A. *J. Chem. Soc., Dalton Trans.* **1985**, 1195.
- Barbucci, R.; Casolaro, M.; Danzo, N.; Barone, V.; Ferruti, P.; Angeloni, A. *Macromolecules* **1983**, *16*, 456.
- Ishiyama, M.; Tominaga, H.; Shiga, M.; Sasamoto, K.; Ohkura, Y.; Ueno, K. *Biol. Pharm. Bull.* **1996**, *19*, 1518.
- Gallagher, J. A.; Gundle, R.; Beresford, J. N.; Isolation and Culture of bone-forming cells (osteoblast) from human bone. In *Human Cell Culture Protocols*; Jones, G. E., Ed.; Humana Press: Totowa, New Jersey; 1996; pp 233–262.
- Ferruti, P.; Knobloch, S.; Ranucci, E.; Duncan, R.; Gianasi, E. *Macromol. Chem. Phys.* **1998**, *199*, 2565.
- Moedritzer, K.; Irani, R. R. *J. Inorg. Nucl. Chem.* **1961**, *22*, 297.
- Grabenstein, R. J.; Quimby, O. T.; Flautt, T. J. *J. Phys. Chem.* **1967**, *71*, 4194.
- Morawetz, H. In *Macromolecules in Solution*; Wiley-Interscience: New York, 1980.
- Ferruti, P.; Barbucci, R. *Adv. Polym. Sci.* **1984**, *58*, 55.
- Casolaro, M.; Chelli, M.; Ginanneschi, M.; Laschi, F.; Messori, L.; Muniz-Miranda, M.; Papini, A. M.; Kowalik-Jankowska, T.; Kozlowsky, H. *J. Inorg. Biochem.* **2002**, *89*, 181.
- Barbucci, R.; Casolaro, M.; Ferruti, P.; Nocentini, M. *Macromolecules* **1986**, *19*, 1856.
- Martell, A. E.; Smith, R. M. In *Critical Stability Constants*; Plenum Press: New York, 1974.
- Lin, J. H. *Bone* **1996**, *18*, 75.
- Im, G.; Qureshi, S. A.; Kenney, J.; Rubash, H. E.; Shanbhag, A. S. *Biomaterials* **2004**, *25*, 4105.
- Frediani, B.; Spreafico, A.; Capperucci, C.; Chellini, F.; Gambera, D.; Ferrara, P.; Baldi, F.; Falsetti, P.; Cantucci, A.; Bocchi, L.; Marcolongo, R. *Bone* **2004**, *35*, 859.
- Franchini, J.; Ranucci, E.; Ferruti, P.; Rossi, M.; Cavalli, R. *Biomacromolecules* **2006**, *7*, 1215.
- Shinoda, H.; Adamek, G.; Felix, R.; Fleisch, H.; Schenk, R.; Hagan, P. *Calcif. Tissue Int.* **1983**, *35*, 87.

BM0607630